

RSC Advances



This is an *Accepted Manuscript*, which has been through the Royal Society of Chemistry peer review process and has been accepted for publication.

Accepted Manuscripts are published online shortly after acceptance, before technical editing, formatting and proof reading. Using this free service, authors can make their results available to the community, in citable form, before we publish the edited article. This *Accepted Manuscript* will be replaced by the edited, formatted and paginated article as soon as this is available.

You can find more information about *Accepted Manuscripts* in the [Information for Authors](#).

Please note that technical editing may introduce minor changes to the text and/or graphics, which may alter content. The journal's standard [Terms & Conditions](#) and the [Ethical guidelines](#) still apply. In no event shall the Royal Society of Chemistry be held responsible for any errors or omissions in this *Accepted Manuscript* or any consequences arising from the use of any information it contains.

A novel high performance oxazine derivative: Design of tetrafunctional monomer, step-wise ring-opening polymerization, improved thermal property and broadened processing window

Cite this: DOI: 10.1039/x0xx00000x

Received
Accepted

DOI:

www.rsc.org/

Tong Zhang^a, Jun Wang^{*a}, Tiantian Feng^a, Hui Wang^a, Nouredine Ramdani^a, Mehdi Derradji^a, Xiaodong Xu^a, Wenbin Liu^{*a}, Tao Tang^b

A novel tetraphenol fluorene, 2,7-dihydroxy-9,9-bis-(4-hydroxyphenyl)fluorene (THPF), was synthesized via the condensation reaction of 2,7-dihydroxy-9-fluorenone and phenol in the presence of strong acidic cation exchange resin and 3-mercaptopropionic acid. Thus, a novel tetrafunctional oxazine monomer containing benzoxazine and fluorene-oxazine (t-BF-b) was prepared for the first time by Mannich condensation reaction of THPF with paraformaldehyde and *n*-butylamine. The chemical structures of THPF and t-BF-b were characterized by Fourier transform infrared (FTIR), Elemental analysis, ¹H and ¹³C nuclear magnetic resonance (NMR). The viscosity-temperature property and the polymerization behavior of t-BF-b as well as the thermal and mechanical properties of its cured polymer (poly(t-BF-b)) were studied by rheometer, FTIR, ¹H NMR, differential scanning calorimeter (DSC), thermogravimetric analysis (TGA), and dynamic mechanical analysis (DMA). The results show that poly(t-BF-b) displays a lower melting point and wider processing window. The oxazine rings of fluorene-oxazine possess higher reactivity and lower polymerization temperature than those of benzoxazine. Also, its cured poly(t-BF-b) exhibits higher glass transition temperature than its corresponding bifunctional polybenzoxazines without sacrificing any thermal properties in spite of the introduction of more flexible aliphatic groups into polymer chains.

1. Introduction

Polybenzoxazines, as a new family of thermosetting polymer, exhibit various attractive properties including high thermal stability, high char yields, high glass transition temperature (T_g), near-zero volumetric change upon curing, good mechanical and dielectric properties, low water absorption, and low flammability.¹⁻⁵ These characteristics promote polybenzoxazines over epoxies and traditional phenolic resins in many industries like the electronic encapsulation, composites production, coatings, adhesives, and flame retardant materials. Moreover, bifunctionalized polybenzoxazines are especially outstanding due to their additional molecular design flexibility. To further improve the performance of polybenzoxazines, many strategies have been proposed. By means of increasing the crosslink density of polymer or introducing some

specific functional groups, such as allyl, diacetylene, propargyl, phthalonitrile, nitrile, maleimide, norbornene, oxazoline, benzocyclobutene, etc.,⁶⁻¹³ the thermal properties of polybenzoxazine have been greatly improved. The multiple polymerization processes are also another positive alternative to modify polybenzoxazine by blending with other materials such as epoxy, novolac, polyurethane, bismaleimide, clays, carbon nanotubes, and graphene.^{1-3,14-19}

Besides benzoxazines, naphthoxazines were also synthesized by using hydroxynaphthalene as phenolic precursor to increase the thermal stability and char yield of the resulting thermosets, polynaphthoxazines.^{20,21} Moreover, polybenzoxazines derived from bisphenol and linear aliphatic amine or phenol and linear aliphatic diamine show outstanding mechanical properties and good

processability due to the presence of flexible alkyl chains in their backbones. However, the linear aliphatic amine-based polybenzoxazines generally display low T_g and thermal stability, which decrease with the length of aliphatic chain.^{22,23}

Recently, benzoxazine monomers with multiple oxazine rings have entered our vision. These multi-functional polybenzoxazines or copolymers with epoxy resins, such as triazine-containing polybenzoxazines,^{24,25} phosphorus-containing triamine- and triphenol-based polybenzoxazines with three oxazine rings,^{26,27} displayed good thermal stability and flame-retardant property. Furthermore, a number of studies on benzoxazine/polyhedral oligomeric silsesquioxane (POSS) composites, benzoxazole-based benzoxazine-modified POSS nanocomposite, and branched benzoxazine-containing polysiloxanes were developed.²⁸⁻³³ An improved thermal stability, mechanical properties and humidity resistance of multifunctional star-shaped benzoxazines containing inorganic constituent were synthesized.³⁴⁻³⁶ Two dendritic compounds with pendant benzoxazine were also published.³⁷

Fluorene molecule contains two benzene rings linked with a five-membered ring which provides high overlaps of π -orbitals.³⁸ The polymers containing fluorene moieties in their backbones, such as polyimide, polyamide, epoxy resin, etc., have attracted a considerable attention because of their unique properties such as good heat-resistance, high char yield, good flame retardancy, and excellent solubility in common organic solvent.³⁹⁻⁴¹ Many researches on fluorene-based benzoxazine monomers derived from 9,9-bis-(4-hydroxyphenyl)fluorene (BHPF) and 9,9-bis-(4-aminophenyl) fluorene (BAPF) have been reported.⁴²⁻⁵⁰ Their results showed that the fluorene-based polybenzoxazines display higher T_g and better thermal stability than the bisphenol A-based polybenzoxazines. However, bifunctional fluorene-based polybenzoxazines have some disadvantages such as relatively higher polymerization temperature, low crosslinking density, poor processability, and brittleness of the cured products, although the introduction of aryl ether/ester linkages into the polymer chains, to a certain extent, improved the toughness of the polybenzoxazines.^{49,50} Recently, a novel furan-containing tetrafunctional fluorene-based oxazine monomer with bisphenol- and diamine-type oxazine rings was prepared. The obtained polybenzoxazine exhibits ultrahigh T_g and better thermal stability.⁵¹ However, its preparation needs complex three-step procedures with long reaction time and low yield (ca. 61%). By contrast, this polybenzoxazine is still a brittle polymer because of the introduction of multiple rigid groups into polymer backbone.

As part of our research interest, this study focuses on the preparation of a novel tetrafunctional oxazine monomer in which simultaneously contains benzoxazine and fluorene-oxazine from the reaction of tetraphenol fluorene, 2,7-dihydroxy-9,9-bis(4-hydroxyphenyl)fluorene (THPF), with *n*-butylamine and paraformaldehyde through facile one-step Mannich condensation reaction. The polymerization behavior, viscosity-temperature relation, and thermal properties of the novel oxazine monomer and polymer were evaluated. The difference of oxazine rings ascribed to fluorene-oxazine and benzoxazine was also compared.

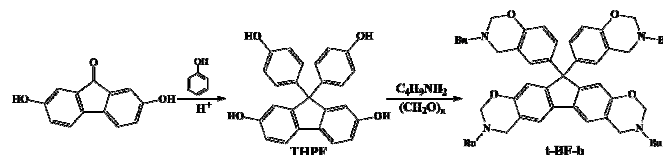
2. Experimental

2.1. Materials

2,7-dihydroxy-9-fluorenone ($\geq 99\%$) was purchased from Wujin Linchuan Chemical Co., Ltd (China). 3-Mercaptopropionic acid was purchased from Sigma-Aldrich. Phenol, paraformaldehyde, and *n*-butylamine were obtained from Shanghai Jingchun Reagent Co., Ltd (China). All solvents were purchased from Tianjin Kermel Chemical Reagent Co., Ltd (China), and used without further purification. Strong acidic cation exchange resin (Amberlyst 121wet) was kindly supplied by Rohm and Haas Shanghai Chemical Industry Co., Ltd, and dried to constant weight in vacuum at 80 °C before using.

2.2. Synthesis of monomer

THPF were synthesized by the reaction of phenol and 2,7-dihydroxy-9-fluorenone in the presence of dried Amberlyst 121wet (acid capacity of 4.8 eq/kg) and 3-mercaptopropionic acid. Tetraphenol fluorene-butylamine-based benzoxazine (t-BF-b) was obtained via Mannich condensation reaction of THPF with paraformaldehyde and *n*-butylamine. The reaction route and the abbreviation of oxazine monomer are shown in Scheme 1.



Scheme 1 Synthetic route to THPF and the target monomer t-BF-b.

2.2.1. Synthesis of THPF

2,7-dihydroxy-9-fluorenone (10.60 g, 0.05 mol), phenol (28.23 g, 0.3 mol), dried Amberlyst 121wet (5.82 g), and 3-mercaptopropionic acid (0.2 mL) were added to a 100 mL three neck round-bottomed flask equipped with a magnetic stirrer, reflux condenser, and thermometer. The mixture was heated at 90-120 °C for 8-11 h. Then, the mixture was separated from ion exchanger by filtration. The recyclable ion exchanger could be reused by washing several times with acetone and dried. The mixture washed several times with hot

water of 65 °C to remove the residual phenol. Then the white precipitate was filtered, recrystallized with 20% ethanol solution, and dried in vacuum at 100 °C for 24 h to afford white crystals (85.6% yield, m.p.: 326 °C by DSC). FTIR (KBr, cm⁻¹): 3378 (O–H stretching), 1609, 1509, and 1451 (aromatic skeletal vibration), 1232 and 1175 (C–O stretching). ¹H NMR (500 MHz, DMSO-d₆, ppm): 9.263 (s, 2H, O–H, the protons of fluorene ring), 9.259 (s, 2H, O–H, the protons of benzene rings), 7.49 (d, 2H, fluorene ring–H), 6.88 (d, 4H, benzene ring–H), 6.70 (d, 2H, fluorene ring–H), 6.66 (s, 2H, fluorene ring–H), 6.63 (d, 4H, benzene ring–H). ¹³C NMR (125 MHz, DMSO-d₆, ppm): 156.51–113.08 (24C, the carbons of benzene rings and fluorene ring), 63.64 (1C, the quaternary carbon in fluorene ring). Elem. Anal. Calcd for C₂₅H₁₈O₄: C 78.52%, H 4.74%. Found: C 78.35%, H 4.53%.

2.2.2 Synthesis of t-BF-b

THPF (1.91 g, 5 mmol), paraformaldehyde (1.20 g, 40 mmol), *n*-butylamine (1.46 g, 20 mmol), and 1,4-dioxane (10 mL) were added to a 250 mL three neck flask equipped with a magnetic stirrer, reflux condenser, and thermometer. The mixtures were heated at 100 °C for 6 h. The reaction was then allowed to cool down to room temperature and then poured into deionized water. The crude product was isolated by filtration and washed with deionized water before drying it under vacuum at 60 °C for 24 h. A white powder was obtained (86.2% yield, m.p.: 78 °C). FTIR (KBr, cm⁻¹): 1495 (C–H in-plane bending), 1321 (CH₂ wagging), 1231 (asymmetric stretching of C–O–C), 1139 (C–N–C asymmetric stretching), 1063 (symmetric stretching of C–O–C), 925 (C–H out-of-plane bending). ¹H NMR (500 MHz, CDCl₃, ppm): 6.61–7.26 (m, 10H, Ar–H), 4.83 and 4.78 (s, 8H, O–CH₂–N of fluorene-oxazine and benzoxazine, respectively), 4.03 and 3.83 (s, 8H, Ar–CH₂–N of fluorene-oxazine and benzoxazine, respectively), 2.74 and 2.69 (t, 8H, N–CH₂–), 1.51 and 1.34 (m, 16H, –(CH₂)₂–CH₃), 0.94 and 0.91 (t, 12H, –CH₃). ¹³C NMR (125 MHz, CDCl₃, ppm): 153.22–114.32 (24C, carbons of benzene rings and fluorene ring), 82.66 and 82.31 (4C, O–CH₂–N of fluorene-oxazine and benzoxazine, respectively), 63.93 (1C, quaternary carbon in the fluorene ring), 51.35 and 51.24 (4C, N–CH₂–Ar of fluorene-oxazine and benzoxazine, respectively), 50.70 and 50.55 (4C, N–CH₂–CH₂), 30.25 and 30.23 (4C, CH₂–CH₂–CH₂), 20.38 and 20.36 (4C, CH₂–CH₂–CH₃), 13.98 (4C, –CH₃). Elem. Anal. Calcd for C₄₉H₆₂N₄O₄: C 76.33%, H 8.10%, N 7.27%. Found: C 76.15%, H 7.98%, N 7.19%.

2.3. Polymerization of tetrafunctional oxazine monomer

The synthesized tetrafunctional oxazine monomer containing benzoxazine and fluorene-oxazine was placed into a sheet steel mold, and was degassed under vacuum oven at 80 °C for 4 h to remove embedded gases. Then, the specimens were cured polymerized without any initiator or catalyst according to the following schedule: 160 °C/2 h, 180 °C/3 h, 200 °C/3 h, and 220 °C/2 h in an air-circulating oven with the pressure of 0.1 MPa. The thickness of the cured samples was limited to 2 mm via a polishing process. The following abbreviation will be used for its cured polybenzoxazine: poly(t-BF-b).

2.4. Characterization and Measurements

FTIR spectra were recorded on a Perkin Elmer Spectrum 100 spectrometer in the range of 4000–500 cm⁻¹, which was equipped with a deuterated triglycine sulphate (DTGS) detector and KBr optics. The transmission spectra were obtained at a resolution of 4 cm⁻¹ after averaging four scans by casting a thin film on a KBr plate for the monomer and cured samples. ¹H and ¹³C NMR characterizations were performed using a Bruker AVANCE-500 NMR spectrometer using deuterated chloroform (CDCl₃) or deuterated DMSO (DMSO-d₆) as the solvent and tetramethylsilane (TMS) as an internal standard. The average number of transients for ¹H and ¹³C NMR was 32 and 512, respectively. A relaxation delay time of 1 s was used for the integrated intensity determination of ¹H NMR spectra. Elemental analysis was carried out with a Vario EL cube (Elementar Analysen systeme GmbH). DSC measurements were evaluated by a TA Q200 differential scanning calorimeter under a constant flow of a nitrogen atmosphere of 50 mL/min. The instrument was calibrated using a high-purity indium standard, and α-Al₂O₃ was used as the reference material. About 10 mg of sample was weighed into a hermetic aluminum sample pan at 25 °C, which was then sealed, and the sample was tested immediately. The dynamic scanning experiments ranged from 30 to 350 °C at the heating rate of 20 °C/min. Thermogravimetric analysis (TGA) was done by TA Instruments Q50 at the heating rate of 20 °C/min from 20 to 820 °C under nitrogen atmosphere at a flow rate of 60 mL/min. The dynamic viscosity measurement was performed using an AR-2000ex Rheometer (TA Instruments) at an angular frequency of 6.283 rad/s and in an oscillatory shear mode using a parallel plate (25 mm diameter). The sample was characterized over a temperature range from 30 to 230 °C at the heating rate of 4 °C/min. The dynamic mechanical thermal properties of the cured samples were carried out by a TA Q800 dynamic mechanical analyzer. The rectangular samples (30×5×2 mm³) were loaded in a single-

cantilever mode at the rate of 3 °C/min from 30 to 380 °C with a frequency of 1 Hz under an air atmosphere.

3. Results and discussion

3.1. Synthesis and characterization of THPF

It is well known that bisphenol fluorene can be synthesized from the condensation of 9-fluorenone with phenol in the present of at least one acidic condensation agent. Mineral or organic acids, including H₂SO₄, HCl, *p*-toluenesulfonic acid, and methanesulfonic acid, are usually used as condensation catalysts and 3-mercaptopropionic acid as cocatalyst. However, the above acid-catalysed process requires corrosion resistant materials in contact with process streams and extensive facilities for recovery of the catalyst. In this work, therefore, strong acidic cation exchange resin was used as catalyst to overcome the above problems. Advantages of this methodology are the use of easily handleable, recyclable, and eco-friendly nature of the catalyst. The yield of THPF reached 84.2%-86.7% under optimal process conditions that the molar ratio of phenol to 2,7-dihydroxy-9-fluorenone was 6:1, the mass percentage of dried catalyst was 15% of the total reactants, reaction temperature was 100 °C and reaction time was 10 h. The average yield of THPF reached up to 82.4% under repeated processes.

The structure of THPF was confirmed by FTIR, ¹H and ¹³C NMR, and elemental analysis as shown in Fig. 1-Fig. 3. Comparison the FTIR spectrum of THPF with that of 2,7-dihydroxy-9-fluorenone in Fig. 1, the broad and strong peaks at 3378 cm⁻¹ for THPF assigned to the stretching vibration of phenolic hydroxyl groups can be observed because of the more hydroxyl groups in THPF than that in 2,7-dihydroxy-9-fluorenone. The band peaked at 1701 cm⁻¹ is associated with C=O stretching for 2,7-dihydroxy-9-fluorenone disappears. In Fig. 2, the protons of fluorene ring appear at 6.66, 6.70 and 7.49 ppm, whereas the aromatic protons of benzene rings appear at 6.63 and 6.88 ppm. The doublet at ca. 9.26 ppm is ascribed to the protons of hydroxyl of fluorene ring and benzene rings, respectively. This implies that the property of two kinds of hydroxyl groups may be different. The ¹³C NMR spectrum of THPF in Fig. 3 reveals the presence of the quaternary carbon in fluorene ring located at 63.64 ppm, confirming the successful synthesis of tetraphenol fluorene compound.

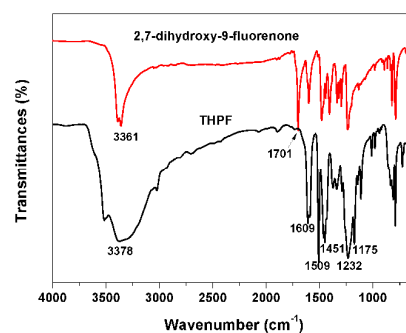


Fig. 1 FTIR spectra of THPF and 2,7-dihydroxy-9-fluorenone.

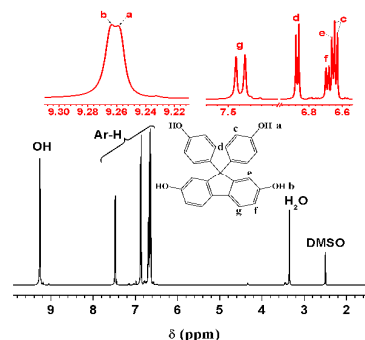


Fig. 2 ¹H NMR spectrum of THPF.

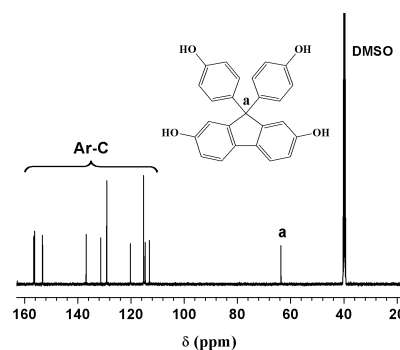


Fig. 3 ¹³C NMR spectrum of THPF.

3.2. Synthesis and structure of t-BF-b

In the previous work, various kinds of bisphenol fluorene-based benzoxazine monomers were obtained utilizing different synthetic strategy as shown in Table 1. We can see that amine and solvent have a greatly influence on the yield of benzoxazine monomers. For example, the yields of bisphenol fluorene-based benzoxazine monomers were below 60% by using mixture of 1,4-dioxane and ethanol as solvent via two-step reaction.⁴⁷ Subsequently, the fluorene-based benzoxazine monomers with higher yield derived from linear and branched butylamine were synthesized by using different solvent via a facile one-step procedure. However, the yield of furfurylamine-based benzoxazine monomer was just 52% under 1,4-dioxane system. The reason is mainly attributed to the polarity of solvent and the basicity of amine.⁴⁸ In this study, 1,4-dioxane was

selected because it can help ring closure of the open Mannich base and especially it can reduce the chances of by-product forming.⁵² In Fig. 4, we can see the peaks localizing at approximately 3.8, 3.6, 2.4, 1.1, and 0.7 ppm in xylene system, which are assigned to the impurities or intermediate products. It was necessary to recrystallize the crude product, leading to the reduction in the final yield of the monomer. *t*-BF-*b* monomer of 86.2% yield was obtained in 1,4-dioxane system while the yield of *t*-BF-*b* monomer was only ca. 60.0% in xylene system. This result is in agreement with the method of reference.⁴⁸

Table 1 Comparison of synthetic approaches for various bisphenol fluorene-based benzoxazine monomers.

Amine	Solvent	Time (h)	Temp. (°C)	Yield (wt%)
Aniline ^a	Dioxane/ethanol	6	90	56
<i>o</i> -Toluidine ^a	Dioxane/ethanol	6	90	55
<i>n</i> -Butylamine ^a	Dioxane/ethanol	6	90	54
<i>n</i> -Octylamine ^a	Dioxane/ethanol	6	90	50
<i>n</i> -Butylamine ^b	Dioxane	5	90	86
<i>i</i> -Butylamine ^b	Dioxane	3	100	81
<i>s</i> -Butylamine ^b	Toluene	1	90	74
<i>t</i> -Butylamine ^b	Toluene	1	100	86
Aniline ^c	Xylene	2	130	78
Allyamine ^c	Xylene	2	130	74
Furfurylamine ^d	Dioxane	36	105	52

a Data from reference 47; b Data from reference 48;

c Data from reference 42; d Data from reference 45.

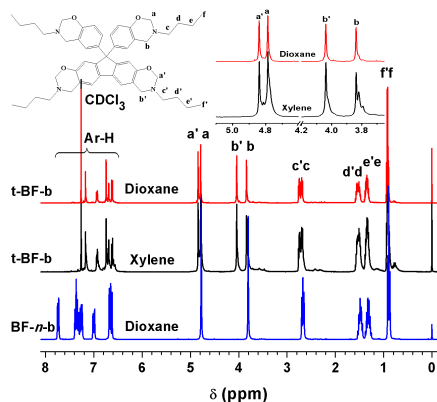


Fig. 4 Comparison of ¹H NMR spectra of BF-*n*-*b* and *t*-BF-*b* synthesized in different reaction media.

The structure of *t*-BF-*b* was also characterized by FTIR, ¹H and ¹³C NMR, and elemental analysis. In Fig. 4, we can see four peaks at 3.83-4.83 ppm, which are due to the CH₂ protons on oxazine rings of fluorene-oxazine and benzoxazine, respectively. This result confirms

the existence of two kinds of oxazine rings ascribed to fluorene-oxazine and benzoxazine, respectively. In order to identify the various shifts of protons in oxazine rings, Fig. 4 compares the ¹H NMR spectra of the bifunctional fluorene-based benzoxazine monomer (BF-*n*-*b*) and *t*-BF-*b*. It can be found that the protons of oxazine rings attached to benzene rings appear in the same chemical shift, while the peaks of oxazine rings attached to fluorene ring shift to a lower field. Simultaneously, all the chemical shift values of methyl and methylene in butyl groups connected to the oxazine ring of fluorene-oxazine also appear at field higher than those for benzoxazine. The ¹³C NMR spectrum is a supplementary evidence of the structure as shown in Fig. 5. The resonances at 114.32-153.22 ppm are ascribed to the aromatic carbons. The chemical shift at 63.93 ppm is attributed to the quaternary carbon atom on the fluorene. The doublets located at ca. 82.5 and 51.3 ppm are attributed to the carbon atom of O-CH₂-N and Ar-CH₂-N of oxazines attached to fluorene and benzene rings, respectively. The doublets of methyl and methylene groups connected to fluorene-oxazine and benzoxazines, respectively, are also observed at 13.98-50.70 ppm, indicating the differences between fluorene-oxazine and benzoxazine in structure.

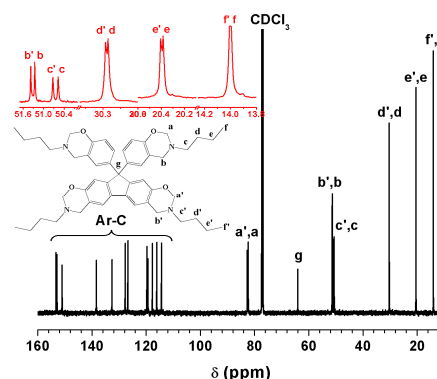


Fig. 5 ¹³C NMR spectrum of *t*-BF-*b*.

The FTIR spectrum of *t*-BF-*b* further evidences the expected structure. As can be seen in Fig. 6 for monomer, the band at 1495 cm⁻¹ is corresponded to the 1,2,4-trisubstituted of benzene ring. The absorption at 1321 cm⁻¹ is attributed to the CH₂ wagging on oxazine rings. The asymmetric and symmetric stretching vibrations of C-O-C located at 1231 and 1063 cm⁻¹ and the asymmetric stretching vibration of C-N-C located at 1139 cm⁻¹, respectively, are observed. The peak at 925 cm⁻¹, which is ascribed to the characteristic mode of the oxazine ring attached to benzoxazine, indicates that the monomer containing oxazine structure is obtained.^{45,47,53-56} The elemental analysis also shows that the measured values of *t*-BF-*b* are in agreement with the calculated

values, confirming the successful synthesis of the tetrafunctional oxazine compound containing benzoxazine and fluorene-oxazine.

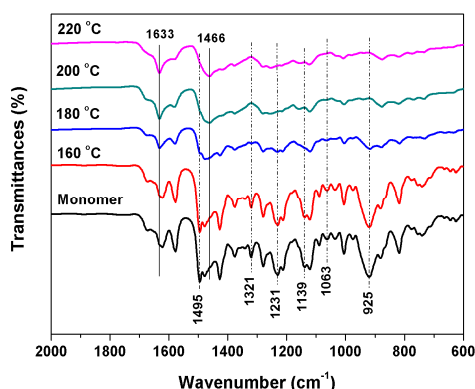


Fig. 6 FTIR spectra of t-BF-b and cured sample recorded at different polymerization stages from 160 to 220 °C for each 2 h.

3.3. Polymerization behavior of t-BF-b

The polymerization behavior of t-BF-b was studied by FTIR, ^1H NMR and DSC. The FTIR spectra of t-BF-b at different curing stages are depicted in Fig. 6. The characteristic absorption bands associated with the oxazine ring, CH_2 wagging, the asymmetric and symmetric stretching of $\text{C}-\text{O}-\text{C}$ and tri-substituted benzene ring are gradually decreased with the increasing polymerization temperature, and are completely disappeared at 220 °C, indicating the completion of ring-opening process at this stage. Meanwhile, the other cross-linking reaction such as substitution can be found. The new absorption at 1466 cm^{-1} is attributed to 1,2,3,5-tetra-substituted benzene ring, showing that the Mannich bridge linkage is produced by the oxazine-ring opening polymerization at the elevated temperature.^{55,57} The asymmetric stretching mode of $\text{C}-\text{N}-\text{C}$ shifts to 1155 cm^{-1} . The band at 1633 cm^{-1} is attributed to intramolecular hydrogen bonded phenolic OH produced by the ring-opening of the tetraphenol-based oxazine.^{46-48,57}

The ring-opening polymerization of benzoxazine is thought to proceed via cationic mechanism.⁵⁸⁻⁶³ In order to get better understanding of the ring-opening polymerization of this type of the tetrafunctional oxazine containing benzoxazine and fluorene-oxazine, we compare the change of the CH_2 proton signals of two oxazine rings for the cured t-BF-b samples. Fig. 7 shows the spectra of ^1H NMR in the region of 5.3-3.6 ppm for t-BF-b before and after polymerization at 160 °C from 30 to 120 min with an interval of 30 min. The integral values of each CH_2 proton of oxazine rings on the basis of methyl group are summarized in Table 2. We can see that the intensities and integrals of the characteristic peaks, which are attributed to the protons of $\text{O}-\text{CH}_2-\text{N}$ and $\text{Ar}-\text{CH}_2-\text{N}$, decrease

with the increasing of polymerization time. By contrast, the variation of the oxazine rings attached to fluorene-oxazine is much higher than that attached to benzoxazine, indicating that the opening of oxazine rings attached to fluorene-oxazine are prior to those attached to benzoxazine. This result implies that the oxazine rings attached to fluorene-oxazine display higher reactivity than those attached to benzoxazine, which may be due to the higher electron density of fluorene moiety. Thus, the benzoxazine polymerization is autocatalyzed as the newly produced phenolic structure acts as an additional initiator and catalyst.

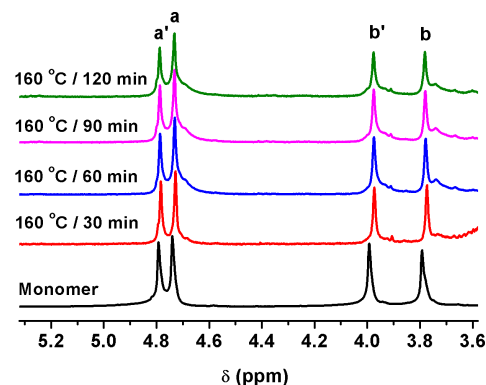
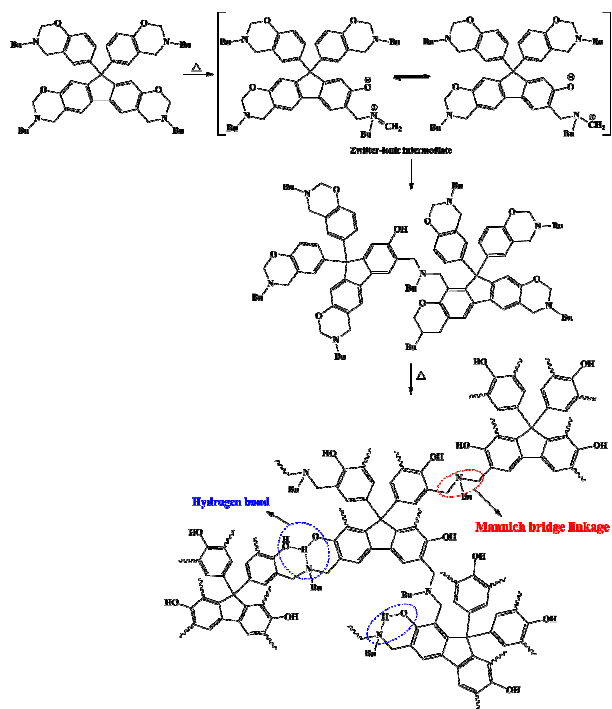


Fig. 7 ^1H NMR spectra of t-BF-b in CDCl_3 and the cured samples in deuterated DMSO at 160 °C for 30-120 min.

Table 2 The integrals of each CH_2 proton at different polymerization stages.

Samples	Integrals			
	a'	a	b'	b
Monomer	0.9926	0.9916	0.9957	0.9959
160 °C/0.5 h	0.7263	0.9446	0.7857	0.9777
160 °C/1.0 h	0.5215	0.9338	0.5735	0.9410
160 °C/1.5 h	0.4860	0.7797	0.4931	0.7894
160 °C/2.0 h	0.4759	0.7173	0.4661	0.6963

Based on these experimental results and comprehensive survey, we proposed a stepwise ring-opening polymerization mechanism and possible polymer network structure for the tetrafunctional oxazine containing benzoxazine and fluorene-oxazine shown in Scheme 2.



Scheme 2 Proposed polymerization mechanism and polymer network structure for t-BF-b.

The non-isothermal DSC thermograms of t-BF-b sample at each polymerization stage are shown in Fig. 8. The broad exotherm with an onset at 212 °C, which is lower than that of the corresponding bifunctional fluorene-based benzoxazine monomer (BF-*n*-b, 221 °C), can be observed.⁴⁸ The peak temperature of polymerization exotherm at 261 °C of t-BF-b is close to BF-*n*-b (256 °C) and the typical benzoxazine, which is due to the thermal polymerization characteristic of oxazine ring-opening. The melting endotherm peak appears at 78 °C, which is much lower than that of BF-*n*-b (173 °C).

Moreover, the amount of exotherm of the sample gradually decreases with the polymerization temperature, while the degree of polymerization is gradually raised. When the sample is cured at 160–200 °C, the degree of polymerization attains 61.6%, 88.8%, and 95.7%, respectively, which is similar to the results by ¹H NMR. The polymerization reaction completes at 220 °C. In this stage, the step-like change in the thermogram is corresponding to the glass transition.

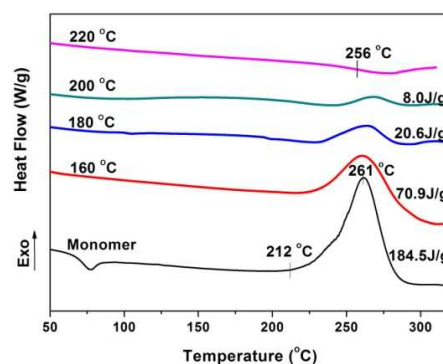


Fig. 8 DSC thermograms of t-BF-b at each cure stage.

3.4. Viscosity-temperature property of t-BF-b

The rheological analysis was used to further understand the viscoelasticity and processability of t-BF-b and its polymer. The variation in viscosity of resin due to changes in temperature or time is regarded as the processing window of the resin shown in Fig. 9. The viscosity of t-BF-b initially decreases due to heating past its liquefying or softening point to reach its minimum value of 0.16 Pa·s at 160 °C. t-BF-b can conveniently be processed or transferred into the mold. Then, with the increase of temperature, the viscosity of t-BF-b increases through the polymerization process past its gel point and the material is transformed into an infusible solid. This is due to the fact that beyond the gel point, which is associated with the appearance of equilibrium modulus or solid-like viscoelastic behavior. The material is unable to flow easily and, therefore, this directly affects processability.⁶⁴ The processing window of t-BF-b, from ca. 65 to 210 °C, exceeds those of traditional bisphenol-A based benzoxazine and bifunctional fluorene-based benzoxazine.^{48, 65} The more flexible butyl chains are beneficial to increase the mobility of polymer segments and improve its processing property.

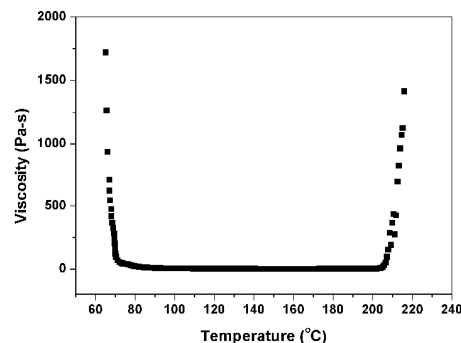


Fig. 9 Viscosity as a function of temperature for t-BF-b in non-isothermal model.

3.5. Thermal and mechanical properties of poly(t-BF-b)

Dynamic mechanical property of poly(t-BF-b) was examined by DMA as shown in Fig. 10. It can be clearly seen in Fig. 8 and Fig.

10 that the T_g value of poly(t-BF-b) attains 256 °C by DSC and 276 °C by DMA, respectively, in spite of the introduction of more flexible aliphatic chains, which is much higher than that of the most bifunctional polybenzoxazine without specific functional groups as shown in Table 3. As we know, T_g and thermal stability of polymer are affected by the backbone rigidity of the polymers, cross-linking density and hydrogen-bonding networks.⁶⁶ Compared with those bifunctional bisphenol- and diamine-based polybenzoxazines, the introduction of more oxazine rings and rigid fluorene groups into oxazine structure can greatly increase the crosslink density of polymer and the rigidity of polymer skeleton. The rigid fluorene groups located in the main chain avoid hanging in the network structure for poly(t-BF-b), sequentially lower the free volume of polybenzoxazine.⁵¹ Furthermore, the strong intramolecular and intermolecular hydrogen bonding produced by the ring-opening of the benzoxazine and fluorene-oxazine results in the tighter packing of polymer chains, which restrains the internal rotations and thermal motion of polymer segments. Therefore, this type of tetrafunctional oxazine compound containing benzoxazine and fluorene-oxazine displays high T_g value. In addition, the storage modulus value of poly(t-BF-b) is 1.91 GPa at 50 °C, which is close to that of traditional bisphenol A-based polybenzoxazine. However, the storage modulus sharply decreases with the increasing temperature, indicating an increase in the flexibility and the chain mobility within this thermoset during the heat treatment.

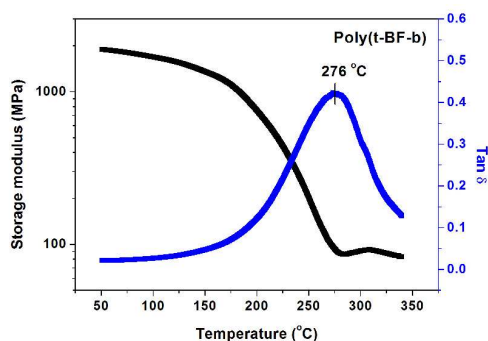


Fig. 10 Temperature dependence curves of storage modulus and tan delta for poly(t-BF-b).

Thermal stability was evaluated by TGA under a nitrogen atmosphere. In Fig. 11, the initial decomposition temperatures corresponding to 5% and 10% weight loss (T_5 and T_{10}) are 326 and 342 °C, respectively, and the char yield at 800 °C is 37.0%, which are higher than those of poly(BF-*n*-b) and poly(BA-a) (Table 3) despite the incorporation of more flexible chains into polymer

network.⁴⁸ This improvement can also be ascribed to the high crosslink density and tight packing of poly(t-BF-b).

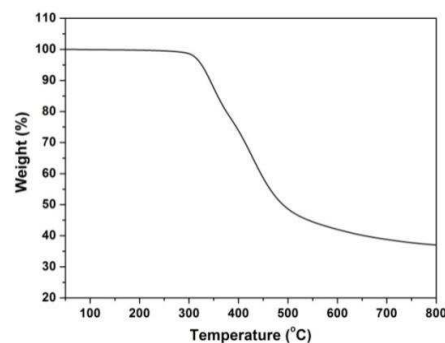


Fig. 11 TGA thermogram of poly(t-BF-b) under nitrogen atmosphere.

Table 3 Thermal properties of difunctional polybenzoxazines.

Bisphenols or diamines	Amine or phenol	T_g (°C) ⁱ	T_5 (°C)	Char Yield (%) ^j
Bisphenol fluorene	Aniline ^a	229	334	51
	<i>o</i> -Toluidine ^a	226	337	52
	<i>n</i> -Octylamine ^a	203	316	19
	<i>n</i> -Butylamine ^b	178	304	33
	<i>i</i> -Butylamine ^b	184	309	39
	<i>s</i> -Butylamine ^b	224	329	44
	<i>t</i> -Butylamine ^b	199	331	45
Bisphenol A	Furfurylamine ^c	215	384	56
	Aniline ^d	217	331	45
Fluorene diamine	Aniline ^e	170	310	32
	<i>n</i> -Butylamine ^f	135	--	--
DDM	Phenol ^g	256	401	49
	<i>o</i> -Cresol ^g	244	372	43
DDS	Salicylide ^h	208	425	52
	Salicylide ^h	184	382	62

a Data from reference 47; b Data from reference 48; c Data from reference 45 (T_g measured by DMA; T_{10} =384 °C; char yield at 900 °C); d Data from reference 42; e Data from reference 1; f Data from reference 66; g Data from reference 46 (T_g measured by DMA); h Data from reference 67 (DDM: 4,4'-diamino diphenyl methane; DDS: 4,4'-diamino diphenyl sulfone); i Measured by DSC; j char yield at 800 °C in nitrogen.

Conclusions

A novel tetrafunctional oxazine monomer containing both benzoxazine and fluorene-oxazine has been successfully synthesized for the first time via facile one-step Mannich condensation reaction. The polymerization behavior and viscosity-temperature property of

t-BF-b and the thermal and thermomechanical properties of its polymer are also investigated. The results show that the viscosity of t-BF-b initially decreases and dramatically increases with the increasing temperature, indicating that this type of oxazine monomer containing benzoxazine and fluorene-oxazine exhibits good processability and broad processing window of ca. 145 °C. The fluorene-oxazine possesses higher reactivity and lower curing temperature than benzoxazine. Its cured polymer displays the high T_g and the improved thermal stability without sacrificing any thermal properties. In comparison to the traditional poly(BA-a) and poly(BF-n-b), the T_g , T_5 , and the char yield at 800 °C values increase 78-106 °C, 16-22 °C, and 4.1-5.0%, respectively, attributed to the introduction of rigid fluorene group, high cross-linking density, and abundant hydrogen bond. All these characteristics make this type of the novel tetrafunctional oxazine polymer suitable for high performance composite matrices, laminate materials, electronic encapsulation materials and fire resistant materials.

Acknowledgements

The authors greatly appreciated the financial supports from National Natural Science Foundation of China (Project No. 50973022), Specialized Research Funds for the Doctoral Program of Higher Education (Project No. 20122304110019), Fundamental Research Funds for the Central Universities (Project No. HEUCFT1009), and the Open Research Fund of State Key Laboratory of Polymer Physics and Chemistry, Changchun Institute of Applied Chemistry, Chinese Academy of Sciences.

Notes and references

^a Polymer Materials Research Centre, Key Laboratory of Superlight Material and Surface Technology of Ministry of Education, College of Materials Science and Chemical Engineering, Harbin Engineering University, Harbin 150001, PR China.

^b State Key Laboratory of Polymer Physics and Chemistry, Changchun Institute of Applied Chemistry, Chinese Academy of Science, Changchun 130022, PR China.

- H. Ishida and T. Agag, *Handbook of Benzoxazine Resins*, 2011.
- Y. Yagci, B. Kiskan and N. N. Ghosh, *J. Polym. Sci., Part A: Polym. Chem.*, 2009, **47**, 5565-5576.
- N. N. Ghosh, B. Kiskan and Y. Yagci, *Prog. Polym. Sci.(Oxford)*, 2007, **32**, 1344-1391.
- M. A. Espinosa, M. Galià and V. Cádiz, *Polymer*, 2004, **45**, 6103-6109.
- S. C. Lin, C. S. Wu, J. M. Yeh and Y. L. Liu, *Polym. Chem.*, 2014, **5**, 4235-4244.
- Y. Cheng, J. Yang, Y. Jin, D. Deng and F. Xiao, *Macromolecules*, 2012, **45**, 4085-4091.
- H. Cao, R. Xu and D. Yu, *J. Appl. Polym. Sci.*, 2008, **110**, 1502-1508.
- H. Ishida and S. Ohba, *Polymer*, 2005, **46**, 5588-5595.
- T. Chaisuwan and H. Ishida, *J. Appl. Polym. Sci.*, 2010, **117**, 2559-2565.
- T. Agag and T. Takeichi, *Macromolecules*, 2003, **36**, 6010-6017.
- H. J. Kim, Z. Brunovska and H. Ishida, *Polymer*, 1999, **40**, 6565-6573.
- T. Agag and T. Takeichi, *Macromolecules*, 2001, **34**, 7257-7263.
- Z. Brunovska, R. Lyon and H. Ishida, *Thermochim. Acta*, 2000, **357-358**, 195-203.
- F. Meng, H. Ishida and X. Liu, *RSC Adv.*, 2014, **4**, 9471-9475.
- K. K. Ho, M. C. Hsiao, T. Y. Chou, C. C. M. Ma, X. F. Xie, J. C. Chiang, S. H. Yang and L. H. Chang, *Polym. Int.*, 2013, **62**, 966-973.
- Y. H. Wang, C. M. Chang and Y. L. Liu, *Polymer*, 2012, **53**, 106-112.
- S. R. Kumar, J. Dhanasekaran and S. K. Mohan, *RSC Adv.*, 2015, **5**, 3709-3719.
- P. Zhao, Q. Zhou, Y. Y. Deng, R. Q. Zhu and Y. Gu, *RSC Adv.*, 2014, **4**, 61634-61642.
- X. Li, Y. Xia, W. Xu, Q. Ran and Y. Gu, *Polym. Chem.*, 2012, **3**, 1629-1633.
- S. B. Shen and H. Ishida, *J. Appl. Polym. Sci.*, 1996, **61**, 1595-1605.
- A. Yildirim, B. Kiskan, A. L. Demirel and Y. Yagci, *Eur. Polym. J.*, 2006, **42**, 3006-3014.
- D. J. Allen and H. Ishida, *Polymer*, 2009, **50**, 613-626.
- T. Agag, A. Akelah, A. Rehab and S. Mostafa, *Polym. Int.*, 2012, **61**, 124-128.
- R. P. Subrayan and F. N. Jones, *Chem. Mater.*, 1998, **10**, 3506-3512.
- D. Wang, B. Li, Y. Zhang and Z. Lu, *J. Appl. Polym. Sci.*, 2013, **127**, 516-522.
- C. W. Chang, C. H. Lin, H. T. Lin, H. J. Huang, K. Y. Hwang and A. P. Tu, *Eur. Polym. J.*, 2009, **45**, 680-689.
- C. H. Lin, S. X. Cai, T. S. Leu, T. Y. Hwang and H. H. Lee, *J. Polym. Sci., Part A: Polym. Chem.*, 2006, **44**, 3454-3468.
- Y. J. Lee, S. W. Kuo, C. F. Huang and F. C. Chang, *Polymer*, 2006, **47**, 4378-4386.
- Y. C. Wu and S. W. Kuo, *Polymer*, 2010, **51**, 3948-3955.
- W. H. Hu, K. W. Huang, C. W. Chiou and S. W. Kuo, *Macromolecules*, 2012, **45**, 9020-9028.
- C. Y. Hsieh, W. C. Su, C. S. Wu, L. K. Lin, K. Y. Hsu and Y. L. Liu, *Polymer (United Kingdom)*, 2013, **54**, 2945-2951.
- K. Zhang, Q. Zhuang, Y. Zhou, X. Liu, G. Yang and Z. Han, *J. Polym. Sci., Part A: Polym. Chem.*, 2012, **50**, 5115-5123.
- K. Zhang, Q. Zhuang, X. Liu, G. Yang, R. Cai and Z. Han, *Macromolecules*, 2013, **46**, 2696-2704.
- B. Kiskan, A. L. Demirel, O. Kamer and Y. Yagci, *J. Polym. Sci., Part A: Polym. Chem.*, 2008, **46**, 6780-6788.
- X. Wu, Y. Zhou, S. Z. Liu, Y. N. Guo, J. J. Qiu and C. M. Liu, *Polymer*, 2011, **52**, 1004-1012.
- X. Wu, S. Z. Liu, D. T. Tian, J. J. Qiu and C. M. Liu, *Polymer*, 2011, **52**, 4235-4245.
- Y. Lu, J. Chen, Y. Lu, P. Gai and H. Zhong, *J. Appl. Polym. Sci.*, 2013, **127**, 282-288.
- L. R. Pattison, A. Hexemer, E. J. Kramer, S. Krishnan, P. M. Petroff and D. A. Fischer, *Macromolecules*, 2006, **39**, 2225-2231.
- M. Ghaemy and M. Barghamadi, *J. Appl. Polym. Sci.*, 2009, **114**, 3464-3471.

40. W. Liu, Q. Qiu, J. Wang, Z. Huo and H. Sun, *Polymer*, 2008, **49**, 4399-4405.
41. S. Kawasaki, M. Yantada, K. Kobori, H. Sakamoto, Y. Kondo, F. Jin and T. Takata, *J. Appl. Polym. Sci.*, 2009, **111**, 461-468.
42. Z. Fu, H. Liu, H. Cai, X. Liu, G. Ying, K. Xu and M. Chen, *Polymer Engineering and Science*, 2012, **52**, 2473-2481.
43. H. C. Chang, C. H. Lin, Y. W. Tian, Y. R. Feng and L. H. Chan, *J. Polym. Sci., Part A: Polym. Chem.*, 2012, **50**, 2201-2210.
44. Y. Lu, M. Li, Y. Zhang, D. Hu, L. Ke and W. Xu, *Thermochim. Acta*, 2011, **515**, 32-37.
45. Y. U. Liu, C. Y. Chang, C. Y. Hsu, M. C. Tseng and C. I. Chou, *J. Polym. Sci., Part A: Polym. Chem.*, 2010, **48**, 4020-4026.
46. J. Wang, X. Y. He, J. T. Liu, W. B. Liu and L. Yang, *Macromol. Chem. Phys.*, 2013, **214**, 617-628.
47. J. Wang, M. q. Wu, W. b. Liu, S. w. Yang, J. w. Bai, Q. q. Ding and Y. Li, *Eur. Polym. J.*, 2010, **46**, 1024-1031.
48. J. Wang, T. T. Ren, Y. D. Wang, X. Y. He, W. B. Liu and X. D. Shen, *React. Funct. Polym.*, 2014, **74**, 22-30.
49. X. Y. He, J. Wang, Y. D. Wang, C. J. Liu, W. B. Liu and L. Yang, *Eur. Polym. J.*, 2013, **49**, 2759-2768.
50. X. Y. He, J. Wang, N. Ramdani, W. B. Liu, L. J. Liu and L. Yang, *Thermochim. Acta*, 2013, **564**, 51-58.
51. H. Wang, J. Wang, X. Y. He, T. T. Feng, N. Ramdani, M. J. Luan, W. B. Liu and X. D. Xu, *RSC Adv.*, 2014, **4**, 64798-64801.
52. H. Ishida and H. Y. Low, *J. Appl. Polym. Sci.*, 1998, **69**, 2559-2567.
53. J. Dunkers and H. Ishida, *Spectrochimica Acta Part A: Molecular Spectroscopy*, 1995, **51**, 1061-1074.
54. P. Larkin, *Infrared and Raman Spectroscopy; Principles and Spectral Interpretation*, 2011.
55. S.-A. Gărea, H. Iovu, A. Nicolescu and C. Deleanu, *Polym. Test.*, 2007, **26**, 162-171.
56. H. Ishida and D. P. Sanders, *Macromolecules*, 2000, **33**, 8149-8157.
57. T. Takeichi, Y. Guo and S. Rimdusit, *Polymer*, 2005, **46**, 4909-4916.
58. A. Sudo, R. Kudoh, H. Nakayama, K. Arima and T. Endo, *Macromolecules*, 2008, **41**, 9030-9034.
59. P. Chutayothin and H. Ishida, *Macromolecules*, 2010, **43**, 4562-4572.
60. R. Andreu, J. A. Reina and J. C. Ronda, *J. Polym. Sci., Part A: Polym. Chem.*, 2008, **46**, 3353-3366.
61. C. Liu, D. Shen, R. M. Sebastián, J. Marquet and R. Schönfeld, *Macromolecules*, 2011, **44**, 4616-4622.
62. X. Wang, F. Chen and Y. Gu, *J. Polym. Sci., Part A: Polym. Chem.*, 2011, **49**, 1443-1452.
63. M. Baqar, T. Agag, R. Huang, J. Maia, S. Qutubuddin and H. Ishida, *Macromolecules*, 2012, **45**, 8119-8125.
64. S. Rimdusit, C. Jubsilp, P. Kunopast and W. Bangsen, in *Handbook of Benzoxazine Resins*, 2011, pp. 143-155.
65. S. Rimdusit, P. Kunopast and I. Dueramae, *Polymer Engineering and Science*, 2011, **51**, 1797-1807.
66. H. Ishida and H. Y. Low, *Macromolecules*, 1997, **30**, 1099-1106.
67. C. H. Lin, S. L. Chang, C. W. Hsieh and H. H. Lee, *Polymer*, 2008, **49**, 1220-1229.

A novel high performance oxazine derivative: Design of tetrafunctional monomer, step-wise ring-opening polymerization, improved thermal property and broadened processing window

Tong Zhang ^a, Jun Wang ^{*a}, Tiantian Feng ^a, Hui Wang ^a, Nouredine Ramdani ^a, Mehdi Derradji ^a, Xiaodong Xu ^a, Wenbin Liu ^{*a}, Tao Tang ^b

